Co-Evolution of Central Black Holes and Galaxies
Proceedings IAU Symposium No. 267, 2009
B. M. Peterson, R. S. Somerville, & T. Storchi-Bergmann, eds.

doi:10.1017/S1743921310006769

Velocity Offsets Due to Mass Outflows in Active Galaxies

D. M. Crenshaw[1], S. B. Kraemer[2], H. R. Schmitt[3], R. F. Mushotzky[4], and J. P. Dunn[5]

[1]Department of Physics and Astronomy, Georgia State University, Astronomy Offices, One Park Place South SE, Suite 700, Atlanta, GA 30303, USA
Email: crenshaw@chara.gsu.edu

[2]Institute for Astrophysics and Computational Sciences, Department of Physics, The Catholic University of America, Washington, DC 20064, USA

[3]Remote Sensing Division, Naval Research Laboratory, Washington, DC 20375; and Interferometrics, Inc., Herndon, VA 20171, USA

[4]NASA/Goddard Space Flight Center, Greenbelt, MD 20771, USA

[5]Department of Physics, Virginia Tech, Blacksburg, VA 24061, USA

Abstract. We present a study of the radial velocity offsets between AGN-related narrow emission lines and host-galaxy emission and absorption lines in Seyfert galaxies with observed redshifts less than 0.043. We find that 35% of the Seyferts in the sample show [O III] emission lines with blueshifts with respect to their host galaxies exceeding 50 km s^{-1}, whereas only 6% show redshifts this large, in qualitative agreement with most previous studies. We also find that a greater percentage of Seyfert 1 galaxies show blueshifts than Seyfert 2 galaxies. Using *HST*/STIS spatially-resolved spectra of the Seyfert 2 galaxy NGC 1068 and the Seyfert 1 galaxy NGC 4151, we generate geometric models of their narrow-line regions (NLRs) and inner galactic disks and show how these models can explain the blueshifted [O III] emission lines in collapsed STIS spectra of these two Seyferts. We conclude that the combination of mass outflow of ionized gas in the NLR and extinction by dust in the inner disk (primarily in the form of dust spirals) is primarily responsible for the velocity offsets in Seyfert galaxies.

Keywords. galaxies: Seyfert, techniques: spectroscopic, line: profiles

1. Introduction

Many AGN show velocity offsets between the emission lines from their narrow-line regions (NLRs) and the stellar absorption lines or H I 21-cm emission from their host galaxies. Comerford *et al.* (2009) present a study in which 32 of 91 Seyfert 2 galaxies with red host galaxies at $0.34 < z < 0.92$ show velocity offsets between their [O III] emission lines and stellar absorption lines that lie in the range ∼50 km s^{-1} to ∼300 km s^{-1}. Comerford *et al.* suggest that the velocity offsets are likely due to displaced AGN that are moving with respect to their host galaxies. They suggest that the most plausible explanation is inspiralling SMBHs after a galaxy merger, which move to the gravitational center of the merger remnant via dynamical friction. They leave open the possibility, however, that the velocity centroids of the emission lines are offset from the systemic velocity of the host galaxy due to a combination of outflows and dust extinction in the NLR. We investigate this issue in more detail using spatially resolved optical spectra of the NLR (∼0.″1 resolution) from the Space Telescope Imaging Spectrograph (STIS) on board the *Hubble Space Telescope (HST).*

2. Analysis of Previous Ground-based Data

We provide a new characterization of the velocity offsets of the narrow lines in Seyfert galaxies, based on the ground-based sample of Nelson & Whittle (1995). From their Table 4, we adopted the stellar absorption velocity ($v_{\rm abs}$) and used the [O III] emission velocity centroid ($v_{\rm em}$) for each AGN to determine the velocity offset: $\Delta v = v_{\rm em} - v_{\rm abs}$. The mean uncertainties of the sample are $15\,{\rm km\,s^{-1}}$ in $v_{\rm abs}$ and $7\,{\rm km\,s^{-1}}$ in $v_{\rm em}$, which added in quadrature yield an uncertainty $\Delta v = 17\,{\rm km\,s^{-1}}$. We consider an offset $\geqslant 3\sigma$, i.e. $|\Delta v| \geqslant 50$ km s^{-1}, to be significant. We identified the AGN in this dataset that are Seyfert galaxies and determined their types using information in NED (placing Seyfert 1.8s and 1.9s into the type 2 category). This yielded a total of 65 Seyfert 1 or 2 galaxies with velocity offsets determined in a uniform manner.

In Figure 1, we plot histograms of the velocity offsets in 50 km s^{-1} bins. The distributions of both Seyfert types peak near zero km s^{-1}, but both show an extended tail on the blueshifted side that goes up to -200 to -250 km s^{-1}. Combining the two histograms, 23/65 (35%) of the Seyferts show blueshifted emission lines with $\Delta v \leqslant -50$ km s^{-1}, whereas 4/65 (6%) of the Seyferts show redshifted lines with $\Delta v \geqslant +50$ km s^{-1}. These results are in agreement with many other studies, which find that the [O III] lines in low-redshift AGN often have blue asymmetries (more flux in the blue side of the profile) and/or blueshifted peaks or centroids with respect to their systemic velocities, whereas few show red asymmetries or redshifted velocity offsets. Comparing the two Seyfert types, the Seyfert 1s are shifted to more negative offset velocities (higher blueshifts, on average) than the Seyfert 2 distribution.

3. Constraints from *HST*/STIS Observations

We have found that the kinematics of the NLR are dominated by radial outflow in the four nearby Seyferts that we have studied to date: NGC 4151 (Hutchings *et al.* 1998; Crenshaw *et al.* 2000; Das *et al.* 2005), NGC 1068 (Crenshaw & Kraemer 2000; Das *et al.* 2006), Mrk 3 (Ruiz *et al.* 2001), and Mrk 573 (T. Fischer *et al.*, in preparation; see also Schlesinger *et al.* 2009). In order to compare our results with those from previous ground-based spectra, we use *HST*/STIS long-slit spectra that cover most of the NLR in NGC 1068 (Cecil *et al.* 2002; Das *et al.* 2006) and NGC 4151 (Das *et al.* 2005). Spectra were

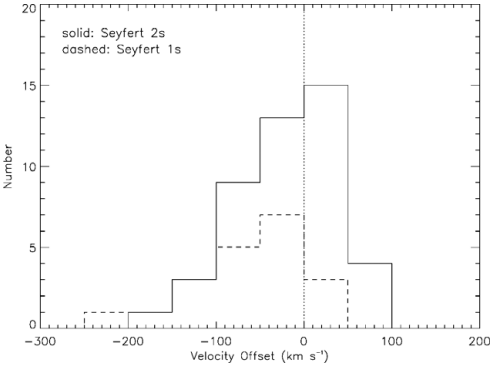

Figure 1. Histograms of the velocity offsets between emission lines and absorption lines ($\Delta v = v_{\rm em} - v_{\rm abs}$) in Seyfert 1 and Seyfert 2 galaxies, from the measurements of Nelson & Whittle (1995).

https://doi.org/10.1017/S1743921310006769 Published online by Cambridge University Press

obtained with the G430M grating through the $52'' \times 0.''2$ slit at a spectral resolving power of $R = \lambda/\Delta\lambda \approx 9000$ and an angular resolution of $\sim 0.''1$ in the cross-dispersion direction. This procedure resulted in hundreds of spectra of the Hβ and [O III] $\lambda\lambda$4959, 5007 lines along each slit position. To simulate the ground-based spectra, we added together all of the spectra along each slit position, and then added together the spectra from each slit.

In Figures 2 and 3, we give these "collapsed" spectra in terms of flux as a function of radial velocity of the [O III] λ5007 line, with respect to the rest frame established by observations of H I 21-cm emission in each galaxy. The unsmoothed profiles in Figures 2 and 3 show significant structure with multiple peaks. From our analysis of the resolved STIS spectra, it is clear that this structure is due to the superposition of velocity profiles from the numerous emission-line knots seen in Figures 2 and 3, with each knot having its own peculiar radial velocity with respect to the general outflow pattern (Das *et al.* 2005, 2006). To simulate low-resolution ground-based spectra at at R =1000, we convolved the unsmoothed spectra with a Gaussian with a FWHM = 500 km s^{-1} (representing the line-spread function) and rebinned them to one-half of a resolution element. These "low-resolution spectra" are also shown in Figures 2 and 3.

The [O III] profiles in Figures 2 and 3 are clearly asymmetric, with more flux in the blue sides of the profiles. In Table 1, we give the heliocentric velocities from the H I 21-cm emission, the stellar absorption lines, and the [O III] measurements described above, as well as the velocity offsets relative to the H I 21-cm velocity. From Table 1, it is clear that the H I 21-cm emission and the stellar absorption features give the same heliocentric velocities, to within the measurement errors of $\sim$10 km s^{-1}. For the [O III] measurements, the velocity centroids are the same to within the errors in both high and low resolution spectra for each galaxy, whereas the velocity peaks are discrepant, particularly for NGC 1068. Thus, the velocity centroids provide a much more reliable measure of the velocity offsets. Looking at the high resolution spectra, the velocity centroids of the [O III] emission are blueshifted by -160 km s^{-1} in NGC 1068 and -60 km s^{-1} in NGC 4151. These fall inside of the range of values for Seyfert galaxies shown in Figure 1, and are what we consider to be significant offsets ($|\Delta v| > 50$ km s^{-1}).

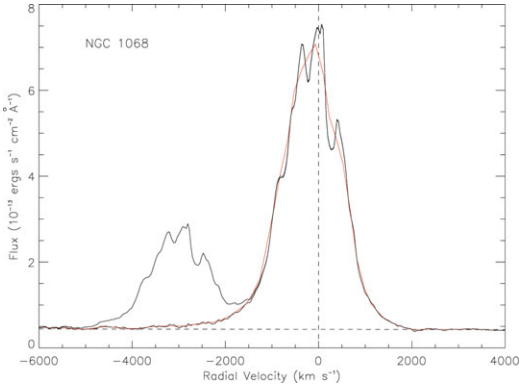

Figure 2. Collapsed spectra of the [O III] emission lines in NGC 1068, obtained by adding together all of the spectra from the STIS long-slit observations and plotting the flux vs. radial velocity, where zero km s^{-1} is defined by H I 21-cm emission. The solid black lines shows the unsmoothed ($R \approx 9000$) spectrum, and the deblended blue wing of [O III] λ5007 underneath the [O III] λ4959 line. The solid gray line shows the heavily smoothed ($R \approx 1000$) version of the [O III] λ5007 line.

https://doi.org/10.1017/S1743921310006769 Published online by Cambridge University Press

Table 1. Heliocentric Radial Velocities and Offsets (in km s^{-1})

H I 21-cm Emission	Stellar Absorption	[O III] High Resolution Centroid	[O III] High Resolution Peak	[O III] Low Resolution Centroid	[O III] Low Resolution Peak
		NGC 1068			
1137 ± 3[a]	1149 ± 8[c]	974 ± 7	1128 ± 5	962 ± 8	988 ± 7
Δv	12 ± 9	-163 ± 8	-9 ± 6	-175 ± 9	-149 ± 8
		NGC 4151			
995 ± 3[b]	1006 ± 18[c]	935 ± 5	998 ± 4	926 ± 3	981 ± 4
Δv	11 ± 18	-60 ± 6	3 ± 5	-69 ± 4	-14 ± 5

Notes:
[a]Bottenelli *et al.* 1990
[b]de Vaucouleurs *et al.* 1991
[c]Nelson & Whittle 1995

4. Geometry of the Outflows and Extinction

To investigate the effects of extinction on mass outflows in the NLR, we assume that the reddening arises from dust in the inner disk of the host galaxy. In order to determine the three-dimensional geometry of the outflows and extinction, we combined our parameters from the biconical outflow models with the observed parameters of the host galaxy disks (Das *et al.* 2005, 2006). In Figure 4, we show the geometry of the biconical outflow and the host galaxy disk for NGC 1068 and NGC 4151. For simplicity, we depict the midplane of the galaxy and the outer surface of the bicone, even though the bicone extends to an inner opening angle in our kinematic models. The left-hand side shows the view from Earth, and the right-hand side shows a viewpoint in which the bicone axis is in the plane of the sky and the galactic disk is edge-on, to show the true angle between the bicone and the disk (see the figure captions for more details). The parallel lines on either side of the galactic midplane show the dust scale height if we assume a typical value of ∼200 pc for spiral galaxies (Xilouris *et al.* 1999) and a length of ∼800 pc for each bicone along its axis (Das *et al.* 2005, 2006).

In the case of NGC 1068, the SW side of the galaxy is closer to us, and the SW cone therefore experiences more extinction. This is consistent with the [O III] image, which

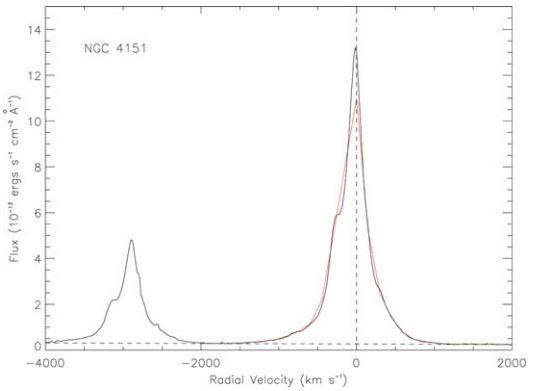

Figure 3. Collapsed spectra of the [O III] emission lines in NGC 4151, obtained by adding together all of the spectra from the STIS long-slit observations and plotting the flux vs. radial velocity, where zero km s^{-1} is defined by H I 21-cm emission. The solid black line shows the unsmoothed ($R \approx 9000$) spectrum. The solid grey line shows the heavily smoothed ($R \approx 1000$) version of the [O III] $\lambda\lambda$4959, 5007 lines.

https://doi.org/10.1017/S1743921310006769 Published online by Cambridge University Press

shows weaker, and in some place absent, emission SW of the location of the SMBH (Das *et al.* 2006). The bicone axis lies nearly in the plane of the sky and the nearer side of each cone is blueshifted, whereas the farther side of each cone is redshifted. Because the disk has a finite thickness, the blueshifted side of each cone in NGC 1068 experiences less extinction, on average, than the redshifted side of each cone. In the case of NGC 4151, the SW cone is entirely blueshifted and the NE cone is entirely redshifted. The host galaxy disk is close to the plane of the sky, and the SW cone shows less extinction than the NE cone shows. Thus, both geometries lead to emission-line profiles that are asymmetric to the blue, in agreement with the observed profiles. As discussed by Crenshaw *et al.* (2009), there are also geometries that lead to a redshifted emission line, although these are relatively rare.

5. Conclusions

We conclude that the velocity offsets of emission lines in low-z Seyfert galaxies are primarily due to a combination of radial outflow in their NLRs and extinction by dust on the same size scale as their NLRs. More exotic explanations are not required. It is

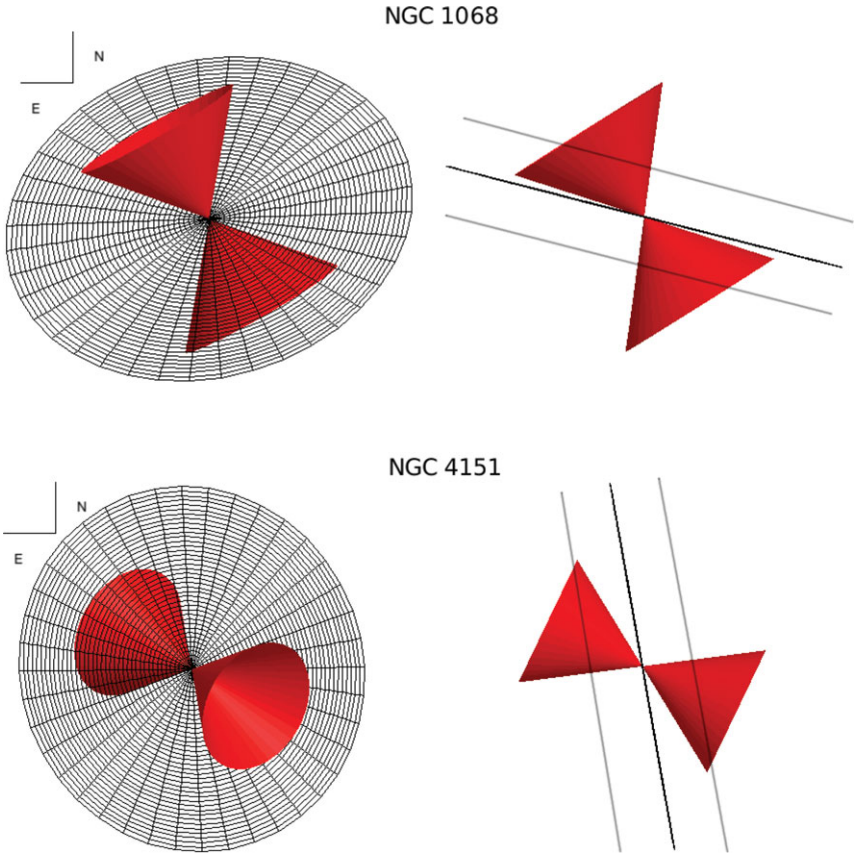

Figure 4. Geometric models of the NLR bicones and the inner galactic disks in NGC 1068 and NGC 4151, based on the parameters in Table 2. The left-hand side shows our view, and the right hand side shows a view in which the bicone axis is in the plane of the sky and the galactic disk is edge-on (our view is to the upper right and above the page for each). The thin gray lines represent a disk scale height of 200 pc for a bicone that is 800 pc in length along its axis.

https://doi.org/10.1017/S1743921310006769 Published online by Cambridge University Press

instructive to compare the distributions of velocity offsets between narrow emission and stellar absorption lines in the low z (< 0.043, Nelson & Whittle 1995) and moderate z ($0.34 < z < 0.92$, Comerford *et al.* 2009) samples. The magnitudes of the velocity offsets in the two distributions are essentially the same, and they have a similar percentage of "significant" ($\geqslant 50$ km s^{-1}) offsets (41% at low z, 35% at moderate z). However, the distribution for the moderate z sample is roughly symmetric around zero km s^{-1}, which is surprising, because these AGN are likely to have outflows in their NLRs as well. In fact, Comerford *et al.* use the symmetric distribution as a reason to disfavor the outflows plus dust explanation and favor the inspiralling black hole scenario. This, in turn, leads them to a merger fraction of ∼30% for red galaxies at these redshifts, which is a surprisinglyarge number, particularly since these galaxies show no evidence for star formation.

The nature of the Comerford *et al.* (2009) sample provides a couple of possible explanations for a symmetric distribution of velocity offsets in the context of mass outflows. Their sample contains only Seyfert 2 galaxies that have been selected to have red host galaxies, to specifically avoid contamination from ionized gas around star-forming regions. The lack of significant star formation suggests a lack of dusty gas, and therefore a lack of extinction, in their NLRs. The velocity offsets would therefore be dominated by uneven distributions of emission-line knots in at least some of the AGN, with no preference for blueshifted profiles. Another possible explanation is that the red colors are due to highly inclined disk galaxies, which will lead to a significant number of redshifts and a more symmetric distribution of velocity offsets. Nevertheless, there is a local example of velocity (and spatial) offsets due to multiple AGN in the nearby galaxy NGC 3341 (Barth *et al.* 2008), and one might expect more of these at higher redshifts from galaxy mergers. Both the low-z and moderate-z samples are rather small; larger sample would be helpful in clarifying the role that mergers might play in producing velocity offsets.

References

Barth, A. J., *et al.* 2008, *ApJ*, 683, L119
Bottinelli, L., *et al.* 1990, *A&AS*, 82, 391
Cecil, G., *et al.* 2002, *ApJ*, 568, 627
Comerford, J. M., *et al.* 2009, *ApJ*, 698, 956
Crenshaw, D. M. & Kraemer, S. B. 2000, *ApJ*, 532, L101
Crenshaw, D. M., *et al.* 2000, *AJ*, 120, 1731
Crenshaw, D. M., *et al.* 2009, *ApJ*, in press [arXiv:0911.0675]
Das, V., *et al.* 2005, *AJ*, 130, 945
Das, V., Crenshaw, D. M., Kraemer, S. B., & Deo, R. P. 2006, *AJ*, 132, 620
de Vaucouleurs, G., *et al.* 1991, *Third Reference Catalogue of Bright Galaxies*, (New York: Springer) (RC3)
Hutchings, J. B., *et al.* 1998, *ApJ*, 492, L115
Komossa, S., Zhou, H., & Lu, H. 2008, *ApJ*, 678, L81
Nelson, C. H. & Whittle, M. 1995, *ApJS*, 99, 67
Ruiz, J., *et al.* 2001 *AJ*, 122, 2961
Schlesinger, K., *et al.* 2009, *ApJ*, 699, 857
Xilouris, E. M., *et al.* 1999, *A&A*, 344, 868.

https://doi.org/10.1017/S1743921310006769 Published online by Cambridge University Press